THE JOURNAL OF BIOLOGICAL CHEMISTRY VOL. 290, NO. 42, pp. 25756–25765, October 16, 2015

Brain-expressed X-linked 2 Is Pivotal for Hyperactive Mechanistic Target of Rapamycin (mTOR)-mediated Tumorigenesis*[S]

Received for publication, May 14, 2015, and in revised form, August 19, 2015 Published, JBC Papers in Press, August 20, 2015, DOI 10.1074/jbc.M115.665208

Zhongdong Hu[‡§], Ying Wang[¶], Fuqiang Huang[‡], Rongrong Chen[‡], Chunjia Li[‡], Fang Wang[‡], June Goto[‖], David J. Kwiatkowski[**], Joanna Wdzieczak-Bakala[‡‡], Pengfei Tu[§], Jianmiao Liu[§§], Xiaojun Zha[¶¶‖‖1], and Hongbing Zhang[‡2]

*From the [‡]State Key Laboratory of Medical Molecular Biology, Department of Physiology, Institute of Basic Medical Sciences and School of Basic Medicine, Graduate School of Peking Union Medical College, Chinese Academy of Medical Sciences and Peking Union Medical College, Beijing 100005, China, the [§]Modern Research Center for Traditional Chinese Medicine, Beijing University of Chinese Medicine, Beijing 100029, China, the [¶]Department of Molecular Orthopaedics, Beijing Institute of Traumatology and Orthopaedics, Beijing Jishuitan Hospital, Beijing 100035, China, the [‖]Division of Pediatric Neurosurgery, Cincinnati Children's Hospital Medical Center, Cincinnati, Ohio 45229, the **Division of Translational Medicine, Department of Medicine, Brigham and Women's Hospital, Harvard Medical School, Boston, Massachusetts 02115, the [‡‡]Institut de Chimie des Substances Naturelles, CNRS UPR2301, 91198 Gif sur Yvette, France, the [§§]Sino-France Laboratory for Drug Screening, Key Laboratory of Molecular Biophysics of Ministry of Education, College of Life Science and Technology, Huazhong University of Science and Technology, Wuhan 430074, China, the [¶¶]Department of Biochemistry and Molecular Biology, School of Basic Medicine, Anhui Medical University, Hefei 230032, China, and the [‖‖]State Key Laboratory Incubation Base of Dermatology, Ministry of National Science and Technology, Hefei 230032, China*

Background: mTOR signaling pathway is frequently activated in cancer.
Results: Hyperactivation of mTOR stimulates STAT3/NF-κB-BEX2-VEGF signaling cascade.
Conclusion: mTOR promotes tumorigenesis through up-regulation of STAT3/NF-κB-BEX2-VEGF signaling axis.
Significance: The components in this mTOR-STAT3/NF-κB-BEX2-VEGF signaling cascade are candidate targets for the treatment of cancers associated with aberrant mTOR signaling.

Frequent alteration of upstream proto-oncogenes and tumor suppressor genes activates mechanistic target of rapamycin (mTOR) and causes cancer. However, the downstream effectors of mTOR remain largely elusive. Here we report that brain-expressed X-linked 2 (BEX2) is a novel downstream effector of mTOR. Elevated BEX2 in *Tsc2*$^{-/-}$ mouse embryonic fibroblasts, *Pten*$^{-/-}$ mouse embryonic fibroblasts, *Tsc2*-deficient rat uterine leiomyoma cells, and brains of neuronal specific *Tsc1* knock-out mice were abolished by mTOR inhibitor rapamycin. Furthermore, BEX2 was also increased in the liver of a hepatic specific *Pten* knock-out mouse and the kidneys of *Tsc2* heterozygous deletion mice, and a patient with tuberous sclerosis complex (TSC). mTOR up-regulation of BEX2 was mediated in parallel by both STAT3 and NF-κB. BEX2 was involved in mTOR up-regulation of VEGF production and angiogenesis. Depletion of BEX2 blunted the tumorigenesis of cells with activated mTOR. Therefore, enhanced STAT3/NF-κB-BEX2-VEGF signaling pathway contributes to hyperactive mTOR-induced tumorigenesis. BEX2 may be targeted for the treatment of the cancers with aberrantly activated mTOR signaling pathway.

Largely due to mutations in either proto-oncogenes or tumor suppressor genes, the receptor tyrosine kinase-phosphoinositide 3-kinase/PTEN-AKT-tuberous sclerosis complex 1/2-mechanstic target of rapamycin (RTK-PI3K/PTEN-AKT-TSC1/2-mTOR)[3] signaling pathway is frequently altered in cancer (1, 2). *PTEN* is a tumor suppressor gene that is mutated in multiple types of human tumors (3). Loss of PTEN activates AKT (4). The potentiated AKT then phosphorylates and inhibits TSC2 (5). TSC1/2 complex serves as a suppressor of mTOR signaling. Inactivation of TSC1/2 complex leads to mTOR hyperactivation and consequently causes tuberous sclerosis complex (TSC), a tumor syndrome affecting multiple organs (6). mTOR is a serine/threonine protein kinase that promotes a subset of protein translation, regulates metabolism, and suppresses autophagy through sensing the state of nutrition and energy, as well as integrating the upstream input (2, 7–10). By

* This work was supported by the National Basic Research Program of China 973 Program (Grant 2015CB553802), the Ministry of Science and Technology of China 863 Program (Grant 2012AA02A201), and the National Natural Science Foundation of China (Grants 81101524, 81130085, 81372475, and 81403147). The authors declare that they have no conflicts of interest with the contents of this article.
[S] This article contains supplemental Table 1.
[1] To whom correspondence may be addressed: Dept. of Biochemistry and Molecular Biology, School of Basic Medicine, Anhui Medical University, 81 Meishan Rd., Hefei 230032, China. E-mail: zhaxiaojunpumc@gmail.com.
[2] To whom correspondence may be addressed: Dept. of Physiology, Institute of Basic Medical Sciences, Peking Union Medical College, 5 Dong Dan San Tiao, Beijing 100005, China. Tel: 86-10-69156491; Fax: 86-10-69156491; E-mail: hbzhang@ibms.pumc.edu.cn or hbzhang2006@gmail.com.

[3] The abbreviations used are: RTK, receptor tyrosine kinase; PTEN, phosphatase and tensin homolog; mTOR, mechanistic target of rapamycin; BEX2, brain-expressed X-linked 2; TSC, tuberous sclerosis complex; TSC1/2, tuberous sclerosis complex 1/2; MEFs, mouse embryonic fibroblasts; CAPE, caffeic acid phenethyl ester; qRT-PCR, quantitative RT-PCR; p, phosphorylated.

associating with different proteins, mTOR participates in the formation of two different complexes: rapamycin-sensitive mTORC1 (composed of mTOR, Raptor, mLST8, DEPTOR, and PRAS40) and rapamycin-resistant mTORC2 (composed of mTOR, Rictor, mLST8, DEPTOR, and mSin1) (2, 11, 12).

Aberrant vascularization is a feature of TSC lesions including facial angiofibroma, retinal hamartomas, cardiac rhabdomyomas, pulmonary lymphangioleiomyomatosis, renal angiomyolipoma, and liver hemangiomas (13). A variety of angiogenesis activating factors have been elucidated, such as basic FGF (bFGF), TGF-α, TGF-β, PDGF, and VEGF. The VEGF serum levels in some cancer patients are elevated (14), and VEGF is a therapeutic target for anti-angiogenesis (15). Studies have revealed that mTOR signaling pathway augments VEGF expression (16–18). However, the underlying mechanism of mTOR up-regulation of VEGF is not completely understood.

Brain-expressed X-linked 2 (BEX2), one of the BEX family members, is abundantly expressed in the central nervous system (19). Evidence has shown that BEX2 is overexpressed in breast cancer (20). BEX2 promotes the growth of breast cancer cells and inhibits mitochondrial apoptosis (21). Reduction of BEX2 expression inhibits angiogenesis *in vivo* (22) and glioma cell migration and invasion (23). Conversely, BEX2 has been found as a tumor suppressor in human glioma because overexpression of BEX2 in glioma cells results in suppression of tumor growth *in vitro* and *in vivo* (24). Hence, the precise function, as well as the regulatory mechanisms, of BEX2 in the development of malignant diseases is still not clear.

In this study, we show that mTOR stimulated BEX2 expression. Hyperactive mTOR promoted carcinogenesis through up-regulation of STAT3/NF-κB-BEX2-VEGF signaling cascade. This study not only unveils an effector in the mTOR signaling pathway, but also reveals a novel mechanism for augmented VEGF expression induced by hyperactive mTOR signaling. In addition, our work provides candidate targets for treatment of cancers associated with aberrant mTOR signaling.

Experimental Procedures

Cell Culture, Reagents, and Plasmids—All mouse embryonic fibroblasts (MEFs) were described previously (25). Retroviral packaging PT67 cells were from Clontech. SK-HEP-1 cells were from Shanghai Institutes for Biological Sciences. A549 and HepG2 cells were from the American Type Culture Collection (Manassas, VA). Bel-7402 cells were from the Cell Institute of the Chinese Academy of Sciences. *Tsc2*-null uterine leiomyoma ELT-3 cells have been reported previously (26, 27). All cells were cultured in DMEM with 10% FBS and 1% penicillin/streptomycin in 5% CO_2 at 37 °C. BEX2 antibody was from Abcam (Cambridge, MA). Anti-phospho-S6 (Ser-235/236) and anti-S6 antibodies have been described previously (28), TSC2, β-actin, and all HRP-labeled secondary antibodies were from Santa Cruz Biotechnology (Santa Cruz, CA). STAT3, p-STAT3 (Tyr-705), p65, p-p65 (Ser-536), mTOR, Raptor, Rictor, and PTEN antibodies were from Cell Signaling Technology (Danvers, MA). VEGF antibody was from Millipore (Billerica, MA). Rapamycin, JSI-124, CAPE, puromycin, and hygromycin B were acquired from Sigma-Aldrich. Lipofectamine 2000 was from Invitrogen. FBS and DMEM were from HyClone (Logan, UT). pBabe-puro and pBabe-STAT3C (control vector and the vector expressing STAT3C (constitutively activated STAT3), respectively) have been reported previously (29). pLXIN-hyg and pLXIN-hTSC2 have been reported previously (30).

Quantitative Real Time PCR—Total RNA was extracted from cells or tissues using TRIzol reagent (Invitrogen). One microgram RNA was reverse-transcribed using the PrimeScript RT reagent kit (TaKaRa, Shiga, Japan). After 10-fold dilution, 4 μl of cDNA was used as the template in a quantitative real time PCR reaction. Amplification was done for 40 cycles using TransStart Green qPCR SuperMix (TransGen Biotech, Beijing, China). Oligonucleotide primers were synthesized to detect BEX2 with β-actin as internal control. The primer sequences are as follows: mouse BEX2, forward: 5′-GCGAGCGGGACAGATTGAC-3′, and reverse, 5′-TCCATTTCTCCTGGGCCTATC-3′; mouse β-actin, forward, 5′-AGAGGGAAATCGTGCGTGAC-3′, and reverse, 5′-CAATAGTGATGACCTGGCCGT-3′.

Expression Profiling Analysis—RNA from WT and $Tsc2^{-/-}$ MEFs was subjected to microarray on an Affymetrix GeneChip system with the Affymetrix Mouse Genome 430 2.0 Array, and data were analyzed using the Partek Express software (31).

Immunoblotting Analysis—Cells were washed with cold PBS, harvested on ice in lysis buffer (2% SDS, 100 mM DTT, 10 mM Tris (pH 6.8), and 10% glycerol), and boiled for 10 min. Cell lysates were resolved by SDS-PAGE. Subsequently, proteins were transferred onto PVDF membrane (Millipore). The membranes were blocked in TBST (0.1 M Tris-Cl (pH 7.5), 0.9% NaCl, 0.5% Tween 20) containing 3% nonfat dry milk at room temperature and incubated with the indicated antibodies diluted with TBST containing 3% nonfat dry milk. After washing with TBST, the membranes were incubated with HRP-labeled secondary antibodies and then detected by chemiluminescence.

Chromatin Immunoprecipitation Assay—Chromatin immunoprecipitation was conducted to examine DNA-protein interactions with an anti-STAT3 antibody and a SimpleChIP® enzymatic chromatin IP kit (Cell Signaling Technology) according to the manufacturer's protocol. The released DNA was purified and then used for analysis by PCR. The primer sequences used for PCR are as follows: the putative STAT3 binding site region of mouse BEX2, forward, ATGCTCTAACAACTGGACTT, and reverse, CTCGACTCAATAGATTTACTC; a nonspecific STAT3 binding region of mouse BEX2, forward, GGTGCTGAATCTTTGAACA, and reverse, ATCCCTTTTGCTAGCATC.

RNA Interference—All the siRNA oligonucleotides were purchased from GenePharma (Shanghai, China). Cells seeded in 6-well plates were transfected with siRNAs (200 nM) in Lipofectamine 2000. Cell lysates were collected for immunoblotting analysis 48 h later. The siRNA target sequences used are as follows: negative control, 5′-TTCTCCGAACGTGTCACGT-3′; TSC2 (human), 5′-CAATGAGTCACAGTCCTTTGA-3′; mTOR (mouse), 5′-GAACTCGCTGATCCAGATG-3′; Raptor (mouse), 5′-AAGGACAACGGTCACAAGTAC-3′; Rictor (mouse), 5′-AAGCCCTACAGCCTTCATTTA-3′; STAT3 (mouse), 5′-CTGGATAACTTCATTAGCA-3′; STAT3 (human), 5′-AACATCTGCCTAGATCGGCTA-3′; p65 (mouse),

5′-GGACCTATGAGACCTTCAA-3′; p65 (human), 5′-GATGAGATCTTCCTACTGT-3′; BEX2 (human), 5′-GCAGGAGAGTTTTACCTAT-3′.

BEX2 Overexpression in WT MEFs—The coding sequence of BEX2 was inserted into PLXIN-hyg vector between XhoI and ClaI sites. PLXIN-hyg-BEX2 and PLXIN-hyg vector were transfected into retroviral packaging PT67 cells using Lipofectamine 2000. After cell selection with hygromycin B (100 μg/ml), cell culture supernatants containing viruses were harvested and filtered with a 0.45-μm filter for subsequent cell infection. Stably expressing cell lines were generated through selection with hygromycin B (100 μg/ml).

BEX2 Knockdown in Tsc2$^{-/-}$ and Pten$^{-/-}$ MEFs—Mouse BEX2 target sequence was inserted into pGPU6/Hyg shRNA expression vector between the BamHI and BbsI sites. The target sequence of mouse BEX2 is 5′-GGAGACTACTACGTGCCTAGA-3′. This construct and the control vector were transfected into *Tsc2*$^{-/-}$ or *Pten*$^{-/-}$ MEFs using Lipofectamine 2000. Stably expressing cell lines were generated through selection with hygromycin B (100 μg/ml).

VEGF ELISA—To determine the levels of VEGF secreted from cells, cells (30,000–40,000 cells/well) were seeded in 12-well plates in triplicates. The next day, culture medium was replaced with 1 ml of fresh medium, and then cells were cultured in 5% CO_2 at 37 °C for 48 h. The number of cells was counted by using a Vi-CELL (Beckman Coulter). Cell culture supernatants were collected, and the secreted VEGF levels in the supernatants were measured with a VEGF ELISA kit (R&D Systems, Minneapolis, MN). The levels of VEGF secretion were normalized to the number of cells (32).

Tumor Engraftment onto Chick Chorioallantoic Membrane—Fertilized chicken eggs were handled as described (33). Briefly, on embryonic day 10, 5,000,000 cells with overexpressed BEX2 or WT cells in 20 μl of culture medium were deposited on chick chorioallantoic membrane. Digital pictures were taken under a stereomicroscope (Nikon SMZ1500) at days 3, 5, and 7 of tumor development.

Induction of Subcutaneous Tumors in Nude Mice—Immunodeficient nude mice (BALB/c, 4–5 weeks old) were purchased from the Institute of Laboratory Animal Science, Chinese Academy of Medical Sciences and Peking Union Medical College. Eight male mice were in each cohort. The subcutaneous tumor model was established as described previously (25, 31).

Human Kidney Tumor Assessment—The kidney angiomyolipoma tissue and adjacent normal tissue from a 16-year-old TSC patient with a frameshift mutation in the *TSC2* gene (g.10059delC, p.S132SfsX50) were extracted with lysis buffer and then subjected to immunoblotting (32). All the procedures were performed under the permission of the Peking Union Medical College Hospital Ethics Board.

Mouse Kidney Tumor Assessment—The kidney cystadenoma tissues and paratumor tissues from four mice with heterozygous deletion of *Tsc2* (34) (*Tsc2*$^{+/-}$, C57BL/6, and 17–18 months old) were extracted with lysis buffer and then subjected to immunoblotting.

Mouse Brain Assessment—WT mice, neuronal specific *Tsc1* knock-out (*Tsc1*$^{f/f}$ *Syn1Cre*) mice, and neuronal specific *Tsc1* knock-out mice treated with rapamycin were sacrificed on postnatal day 21, and brain tissues were extracted with lysis buffer and then subjected to immunoblotting as described previously (35). Total RNA was extracted from the whole brain tissues of WT, and neuronal specific *Tsc1* knock-out mice were sacrificed on postnatal day 13 for qRT-PCR analysis.

TABLE 1
Increased BEX2 in *Tsc2*$^{-/-}$ MEFs
mRNA abundance of BEX2 in WT and *Tsc2*$^{-/-}$ was measured using Affymetrix mouse genome 430 2.0 array.

	Tsc2$^{-/-}$ *vs.* WT	
Gene	-Fold change	Description
Bex2	8.51992	Up

Mouse Liver Assessment—Mice with hepatocyte-specific deficiency of *Pten* were generated by crossing *Pten*$^{f/f}$ mice with *AlbCre* transgenic mice (36). The liver tissues from a WT mouse (*Pten*$^{+/+}$ *AlbCre*, 9 months old) and a liver-specific *Pten*-deficient mouse (*Pten*$^{f/f}$ *AlbCre*, 9 months old) were extracted with lysis buffer and then subjected to immunoblotting (37). All animal protocols were approved by the Animal Center of the Institute of Basic Medical Sciences, Chinese Academy of Medical Sciences and Peking Union Medical College, and were in accordance with the regulation of the Beijing Administration Office of Laboratory Animal on the care of experimental animals.

Statistical Analysis—Mouse tumor development and survival data were analyzed using the Kaplan-Meier log-rank test, and the two-tailed Student's *t* test was used to conduct the comparison between the groups. It was of statistical significance when $p < 0.05$.

Results

Loss of PTEN or TSC2 Potentiates BEX2 Expression—To identify novel targets of TSC2, we extracted mRNA from WT and *Tsc2*$^{-/-}$ MEFs and conducted the gene expression profiling analysis (supplemental Table 1). We found that the abundance of BEX2 was higher in *Tsc2*$^{-/-}$ MEFs than in WT MEFs (Table 1). Quantitative real time PCR revealed that the mRNA level of BEX2 in *Tsc2*$^{-/-}$ MEFs was significantly higher than that of WT MEFs (Fig. 1*A*). Furthermore, the protein level of BEX2 in *Tsc2*$^{-/-}$ MEFs was also increased (Fig. 1*B*). To examine whether the negative regulation of TSC2 on BEX2 exists in human cells, we knocked down TSC2 in human lung adenocarcinoma cell line A549. Reduction of TSC2 resulted in an increase of BEX2 expression in A549 cells (Fig. 1*C*). Moreover, the ectopically expressed human TSC2 in rat uterine leiomyoma cell line ELT3 (*Tsc2*-deficient cells) inhibited BEX2 expression (Fig. 1*D*). Similarly, BEX2 protein was much higher in *Pten*$^{-/-}$ MEFs than in WT MEFs (Fig. 1*E*). Furthermore, the protein level of BEX2 was increased in the mouse liver tissue with hepatocyte-specific *Pten* deletion (Fig. 1*F*). BEX2 was much higher in renal tumor tissues than in adjacent normal renal tissues from *Tsc2*$^{+/-}$ mice (Fig. 1*G*). Moreover, the protein level of BEX2 in renal tumor tissues from a 16-year-old female patient with TSC was higher when compared with adjacent normal renal tissues (Fig. 1*H*).

mTOR Positively Regulates BEX2 Expression—Because deletion of either TSC2 or PTEN leads to mTOR activation (7) and

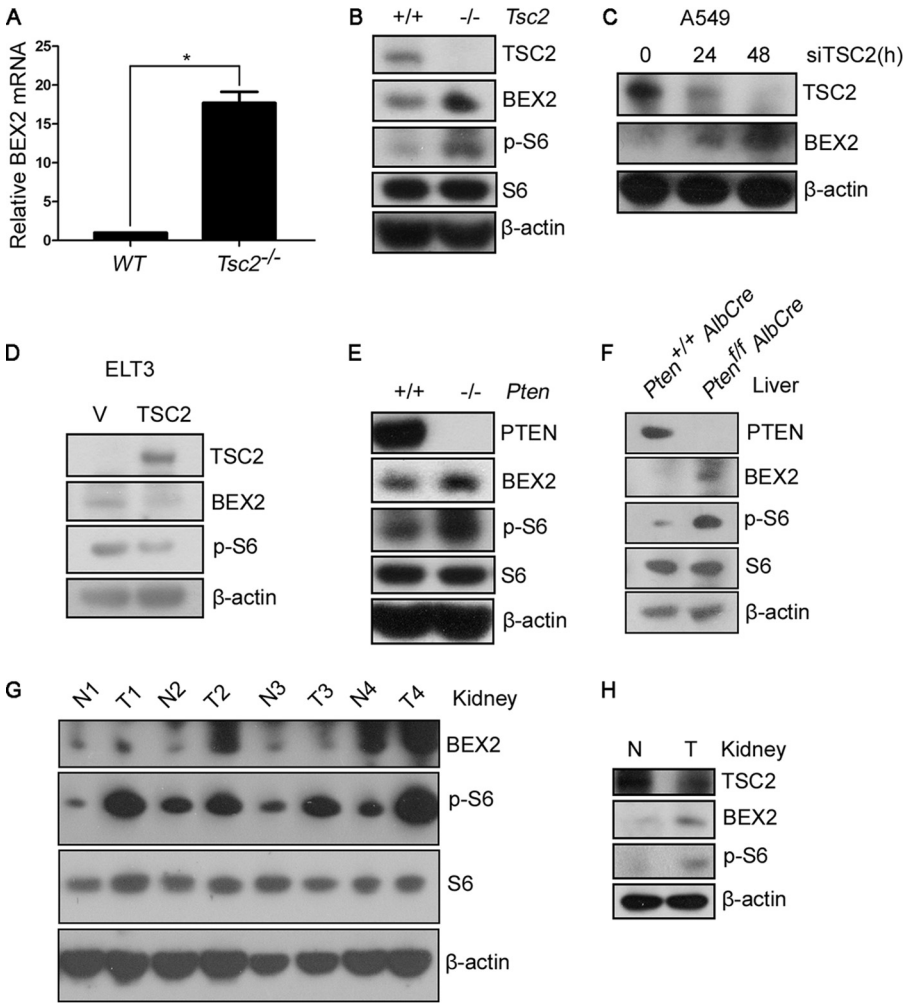

FIGURE 1. **Loss of PTEN or TSC2 potentiates BEX2 expression.** *A* and *B*, total RNA and cell lysates were extracted from WT and $Tsc2^{-/-}$ MEFs for qRT-PCR ($n = 3$, data represent mean ± S.E. *, $p < 0.05$) (*A*) and immunoblotting (*B*). *C*, A549 cells were transfected with control or TSC2 siRNAs (*siTSC2*) for 24 or 48 h and then subjected to immunoblotting. *D*, ELT3 cells were infected with pLXIN-hyg or pLXIN-hTSC2 retroviruses and then subjected to immunoblotting. *V*, vector. *E*, cell lysates were extracted from WT and $Pten^{-/-}$ MEFs for immunoblotting. *F*, age- and genetic background-matched liver tissues dissected from WT mouse ($Pten^{+/+}$ *AlbCre*) and the mutant mouse ($Pten^{f/f}$ *AlbCre*) were subjected to immunoblotting. *G*, kidney cystadenomas (*T*) and paratumor tissues (*N*) from four C57BL/6 $Tsc2^{+/-}$ mice were immunoblotted. *H*, kidney tumor tissue (*T*) and the adjacent normal tissue (*N*) from a TSC patient were immunoblotted.

BEX2 overexpression, we explored whether there is a regulatory relationship between mTOR and BEX2. We treated WT and $Tsc2^{-/-}$ MEFs with the mTOR inhibitor, rapamycin. Rapamycin inhibited BEX2 expression in WT and $Tsc2^{-/-}$ MEFs (Fig. 2, *A* and *B*). A similar change was presented in WT and $Pten^{-/-}$ MEFs with rapamycin treatment (Fig. 2*C*). To test the *in vivo* relevance of this finding, we examined the expression of BEX2 in the brain tissues dissected from WT mice and the neuronal specific *Tsc1* knock-out mice ($Tsc1^{f/f}$ *Syn1Cre*). The level of BEX2 mRNA was elevated in the brain tissues derived from the neuronal specific *Tsc1* knock-out mice over WT mice (Fig. 2*D*). Moreover, the BEX2 protein level was also increased in the neuronal specific *Tsc1* knock-out mice, and the augmented BEX2 was suppressed by rapamycin administration (Fig. 2*E*). BEX2 expression declined after treatment with rapamycin in human liver cancer cell lines (HepG2, Bel-7402, SK-HEP-1), lung adenocarcinoma cell line A549, and rat uterine leiomyoma cell line ELT3 (*Tsc2*-deficient cells) (Fig. 2*F*). To validate mTORC1 in the regulation of BEX2, we knocked down mTOR, Raptor, and Rictor expression in $Tsc2^{-/-}$ MEFs, respectively. Cells transfected with mTOR and Raptor siRNAs had a remarkable decrease in the expression of phospho-S6 and BEX2 (Fig. 2*G*). However, there was no dramatic change in both phospho-S6 and BEX2 expression after knockdown of Rictor, suggesting that BEX2 expression is controlled by mTORC1 instead of mTORC2. Taken together, these data show that mTORC1 is a positive regulator of BEX2 expression.

Reduction of BEX2 Inhibits the Tumorigenic Capacity of Cells with Activated mTOR—To investigate the role of BEX2 in the tumorigenesis of cells with active mTOR, we evaluated the tumorigenicity of $Tsc2^{-/-}$ MEFs expressing shBEX2 or scramble shRNA (shV) in a nude mouse model. Depletion of BEX2 significantly attenuated tumor initiation and progression of $Tsc2^{-/-}$ MEFs in nude mice (Fig. 3*A*). Similarly, knockdown of BEX2 significantly compromised the tumorigenesis of $Pten^{-/-}$ MEFs in nude mice (Fig. 3*B*).

Both STAT3 and NF-κB Participate in mTOR Up-regulation of BEX2 Expression—STAT3 is a transcription factor. Phosphorylation of the tyrosine residue (Tyr-705) is required for activation of STAT3 (38). Activation of STAT3 is detectable in many

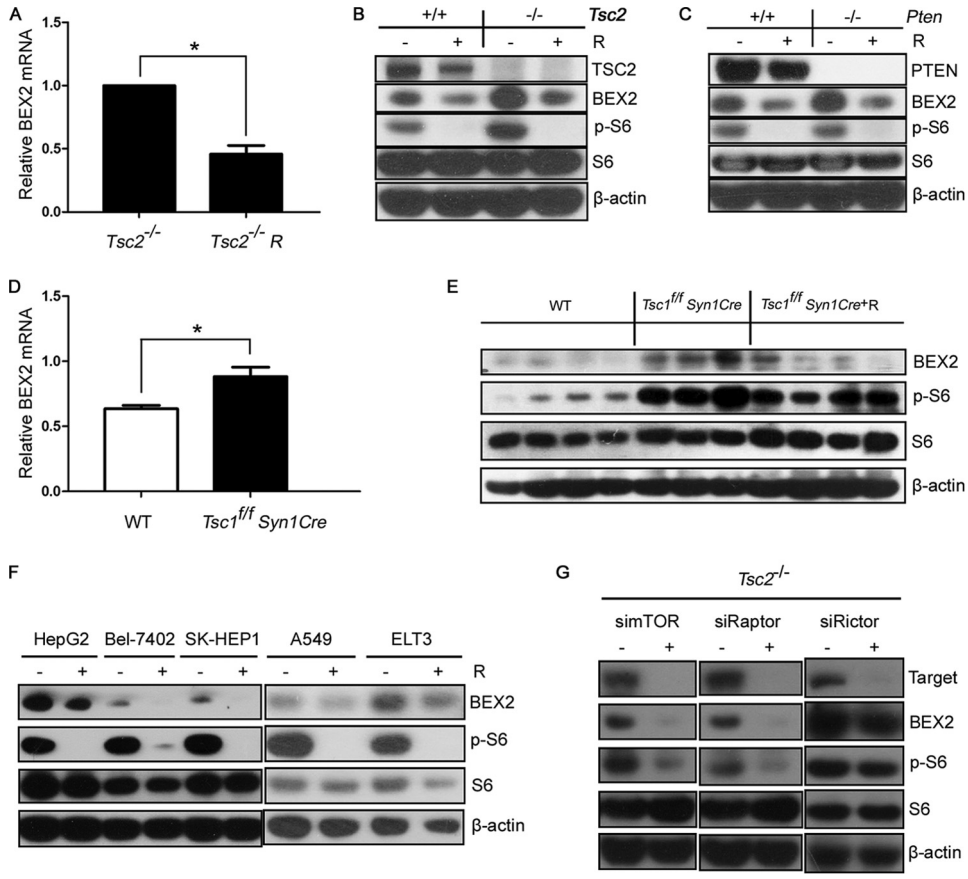

FIGURE 2. **mTOR positively regulates BEX2 expression.** *A*, total RNA were extracted from $Tsc2^{-/-}$ MEFs treated with or without 10 nM rapamycin (*R*) for 24 h for qRT-PCR. $n = 3$, data represent mean ± S.E. *, $p < 0.05$. *B* and *C*, cell lysates were extracted from WT and $Tsc2^{-/-}$ MEFs or $Pten^{-/-}$ MEFs treated with or without 10 nM rapamycin (*R*) for 24 h for immunoblotting. *D*, total RNA was extracted from brain tissues of wild-type mice (*WT*) and the neuronal specific *Tsc1* knock-out mice ($Tsc1^{f/f}$ *Syn1Cre*) for qRT-PCR. $n = 3$, data represent mean ± S.E. *, $p < 0.05$. *E*, the brain tissues from WT mice, $Tsc1^{f/f}$ *Syn1Cre* mice, and $Tsc1^{f/f}$ *Syn1Cre* mice treated with rapamycin (*R*) ($Tsc1^{f/f}$ *Syn1Cre* +R) were immunoblotted. *F*, HepG2, Bel-7402, SK-HEP-1, A549, and ELT3 cells were treated with or without 10 nM rapamycin (*R*) for 24 h and then subjected to immunoblotting. *G*, $Tsc2^{-/-}$ MEFs were transfected with siRNA targeting mTOR (*simTOR*), Raptor (*siRaptor*), or Rictor (*siRictor*) for 48 h and then subjected to immunoblotting.

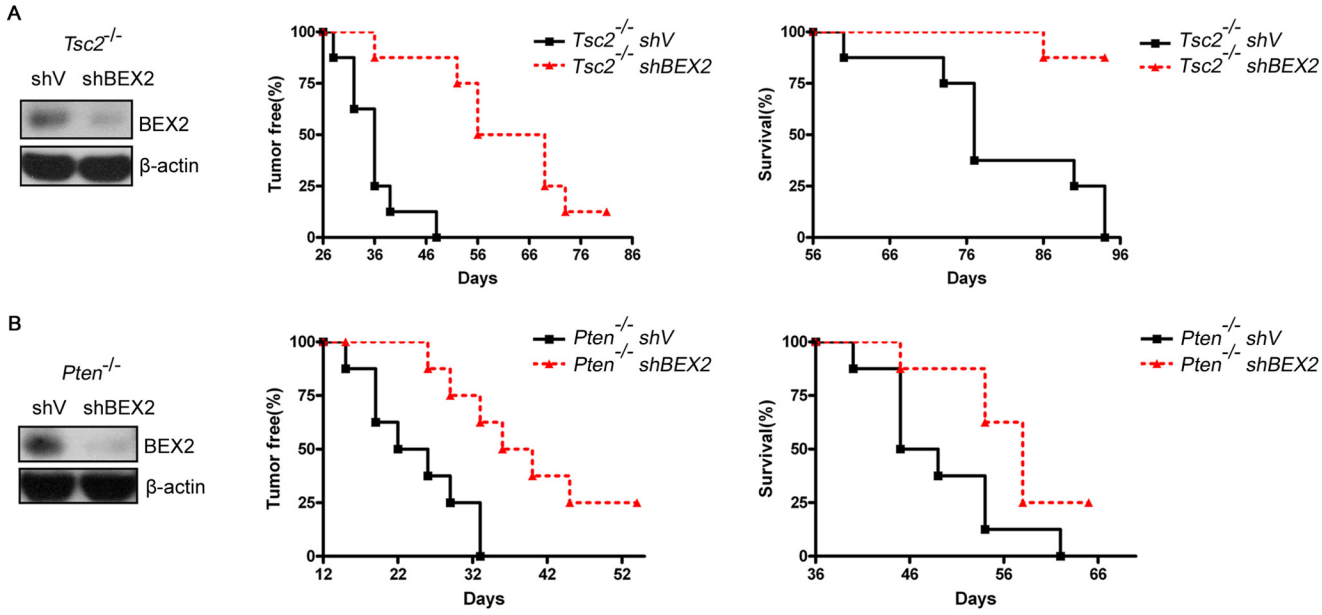

FIGURE 3. **Depletion of BEX2 reduces the tumorigenic capacity of cells with activated mTOR.** *A* and *B*, $Tsc2^{-/-}$ MEFs (*A*) or $Pten^{-/-}$ MEFs (*B*) were transfected with the plasmids (shBEX2 or scramble shRNA (*shV*)) and then inoculated subcutaneously into nude mice ($n = 8$). *Left*: immunoblotting. *Middle*: tumor initiation. *Right*: survival of the mice. Mouse tumor development and survival data were analyzed using the Kaplan-Meier log-rank test, $p < 0.05$.

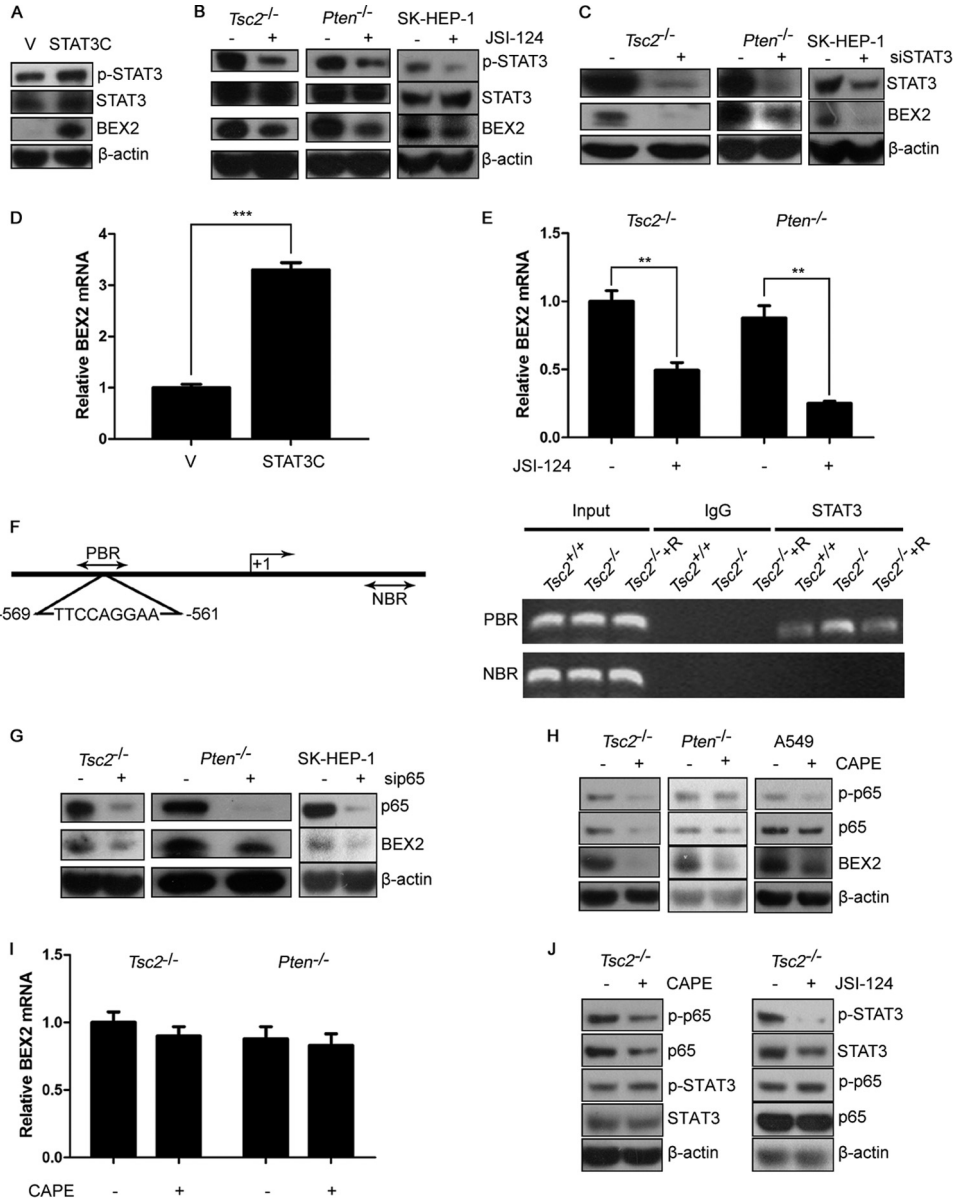

FIGURE 4. **STAT3 and NF-κB up-regulate BEX2 downstream of mTOR.** *A*, WT MEFs transduced with the retroviruses for STAT3C in pBabe-puro or the control vector pBabe-puro (*V*) were subjected to immunoblotting. *B*, $Tsc2^{-/-}$ MEFs, $Pten^{-/-}$ MEFs, or SK-HEP-1 cells were treated with or without JSI-124 ($Tsc2^{-/-}$ MEFs and $Pten^{-/-}$ MEFs, 0.5 μM; SK-HEP-1, 0.1 μM) for 24 h and then subjected to immunoblotting. *C*, $Tsc2^{-/-}$ MEFs, $Pten^{-/-}$ MEFs, or SK-HEP-1 cells were transfected with STAT3 siRNAs for 48 h and then subjected to immunoblotting. *D* and *E*, total RNA were extracted from WT MEFs transduced with the retroviruses for STAT3C in pBabe-puro or the control vector pBabe-puro (*V*) (*D*) and $Tsc2^{-/-}$ MEFs or $Pten^{-/-}$ MEFs treated with or without 0.5 μM JSI-124 for 24 h (*E*) for qRT-PCR. $n = 3$, data represent mean ± S.E. **, $p < 0.01$, ***, $p < 0.001$. *F*, *left*, schematic illustration of a putative STAT3 binding site within the promoter of mouse BEX2 gene. *PBR*, putative STAT3 binding site region; *NBR*, nonspecific STAT3 binding region. *Right*, WT and $Tsc2^{-/-}$ MEFs treated with or without 20 nM rapamycin (*R*) for 24 h were subjected to ChIP assay with an anti-STAT3 antibody. Normal rabbit IgG antibody used as the negative control. Immunoprecipitated DNA was used for PCR amplifications with primers surrounding the putative STAT3 binding site region and nonspecific STAT3 binding region. *G*, $Tsc2^{-/-}$ MEFs, $Pten^{-/-}$ MEFs, or SK-HEP-1 cells were transfected with control or p65 siRNAs (*sip65*) for 48 h and then subjected to immunoblotting. *H*, $Tsc2^{-/-}$ MEFs, $Pten^{-/-}$ MEFs, or A549 cells were treated with or without 10 μM CAPE for 24 h and then subjected to immunoblotting. *I*, total RNA were extracted from $Tsc2^{-/-}$ MEFs or $Pten^{-/-}$ MEFs treated with or without 10 μM CAPE for 24 h for qRT-PCR. $n = 3$, data represent mean ± S.E. $p > 0.05$. *J*, $Tsc2^{-/-}$ MEFs were treated with or without 10 μM CAPE or 0.5 μM JSI-124 for 24 h and then subjected to immunoblotting.

types of tumors (39). Because we have reported that mTOR up-regulates STAT3 (25, 40), we investigated the regulation of BEX2 by STAT3. Overexpression of the constitutively activated STAT3 enhanced BEX2 expression (Fig. 4*A*). To verify this finding, we treated $Tsc2^{-/-}$ MEFs, $Pten^{-/-}$ MEFs, and SK-HEP-1 cells with the STAT3 inhibitor, JSI-124. Inhibition of STAT3 dramatically reduced BEX2 expression in all cell lines examined (Fig. 4*B*). Moreover, suppression of STAT3 with siRNA impaired BEX2 expression in $Tsc2^{-/-}$ MEFs, $Pten^{-/-}$ MEFs, and SK-HEP-1 cells (Fig. 4*C*). In addition, qRT-PCR analysis showed that STAT3C up-regulated BEX2 mRNA expression (Fig. 4*D*). Moreover, the mRNA levels of BEX2 in $Tsc2^{-/-}$ MEFs or $Pten^{-/-}$ MEFs were significantly decreased in the presence of JSI-124 (Fig. 4*E*), indicating that STAT3 regulates BEX2 at the transcriptional level.

To explore whether STAT3 directly transactivates BEX2 gene transcription, we identified a putative STAT3 binding sequence (−569/−561; TTCCAGGAA) within the promoter of

mouse BEX2 gene through the analysis of the 5′-flanking sequence of the BEX2 gene upstream of the transcription start site (Fig. 4*F*, *left*). ChIP analysis revealed that the binding of STAT3 to the putative binding site in the promoter of BEX2 gene was increased in *Tsc2*$^{-/-}$ MEFs when compared with in WT cells. Moreover, the interaction between STAT3 and the BEX2 promoter was decreased after rapamycin treatment (Fig. 4*F*, *right*). Taken together, STAT3 directly promotes the transcription of BEX2 downstream of mTOR.

NF-κB is part of a family of transcription factors, including RelA/p65, c-Rel, RelB, NF-κB1/p50, and NF-κB2/p52 (41), and is constitutively activated in multiple types of tumors (42). NF-κB has been reported locating in the downstream of mTOR (43). To investigate whether BEX2 expression is controlled by NF-κB, we transfected siRNA targeting p65 into *Tsc2*$^{-/-}$ MEFs, *Pten*$^{-/-}$ MEFs, and SK-HEP-1 cells to reduce NF-κB activity. Knockdown of p65 suppressed BEX2 expression in these cells (Fig. 4*G*). Moreover, inhibition of NF-κB with the NF-κB inhibitor, CAPE, resulted in a remarkable reduction of BEX2 protein level in *Tsc2*$^{-/-}$ MEFs, *Pten*$^{-/-}$ MEFs, and A549 cells (Fig. 4*H*). However, the mRNA levels of BEX2 in *Tsc2*$^{-/-}$ MEFs or *Pten*$^{-/-}$ MEFs were not significantly different in the absence or presence of CAPE (Fig. 4*I*). Hence, these results demonstrate that NF-κB positively regulates BEX2 protein level. Our previous study suggests that STAT3 has no regulatory cross-talk with NF-κB (25). In this study, inhibition of NF-κB or STAT3 in *Tsc2*$^{-/-}$ MEFs was unable to affect the activity of either NF-κB or STAT3 (Fig. 4*J*). Therefore, STAT3 and NF-κB stimulate BEX2 expression in parallel downstream of mTOR.

BEX2 Mediates mTOR Augmentation of VEGF Expression—Previous studies have shown that activation of PI3K-AKT-mTOR signaling pathway increases VEGF expression (16, 17, 44). Deficiency in either *Tsc2* or *Pten* indeed led to up-regulation of VEGF, and inhibition of mTOR by rapamycin suppressed the expression of VEGF (Fig. 5, *A* and *B*). To determine whether there was a potential relationship between BEX2 and VEGF, we examined the abundance of VEGF in cell lysates and cell culture supernatants in *Tsc2*$^{-/-}$ MEFs transfected with shRNA targeting BEX2. Suppression of BEX2 expression reduced VEGF expression (Fig. 5*C*) and secretion (Fig. 5*D*) in *Tsc2*-null MEFs. In addition, BEX2 overexpression increased the expression of VEGF in WT MEFs (Fig. 5*E*). To seek the relevance of this finding in human cancer cells, we knocked down BEX2 expression in human hepatocellular carcinoma SK-HEP-1 cells. Reduction of BEX2 suppressed VEGF expression in SK-HEP-1 cells (Fig. 5*F*). Moreover, we examined the effect of BEX2 on angiogenesis through chick chorioallantoic membrane assay. BEX2-overexpressing cells formed more blood vessels, with severe bleeding, than the control cells on day 7 (Fig. 5*G*). Thus, BEX2 mediates mTOR up-regulation of VEGF production and angiogenesis.

mTOR Regulates STAT3/NF-κB-BEX2-VEGF Signaling in Vitro and in Vivo—It was reported that STAT3 and NF-κB positively modulate VEGF expression (45, 46). Likewise, inhibition of STAT3 or NF-κB with JSI-124 or CAPE decreased expression of VEGF in SK-HEP-1, HepG2, and A549 cells, respectively (Fig. 6, *A* and *B*). We next investigated whether this

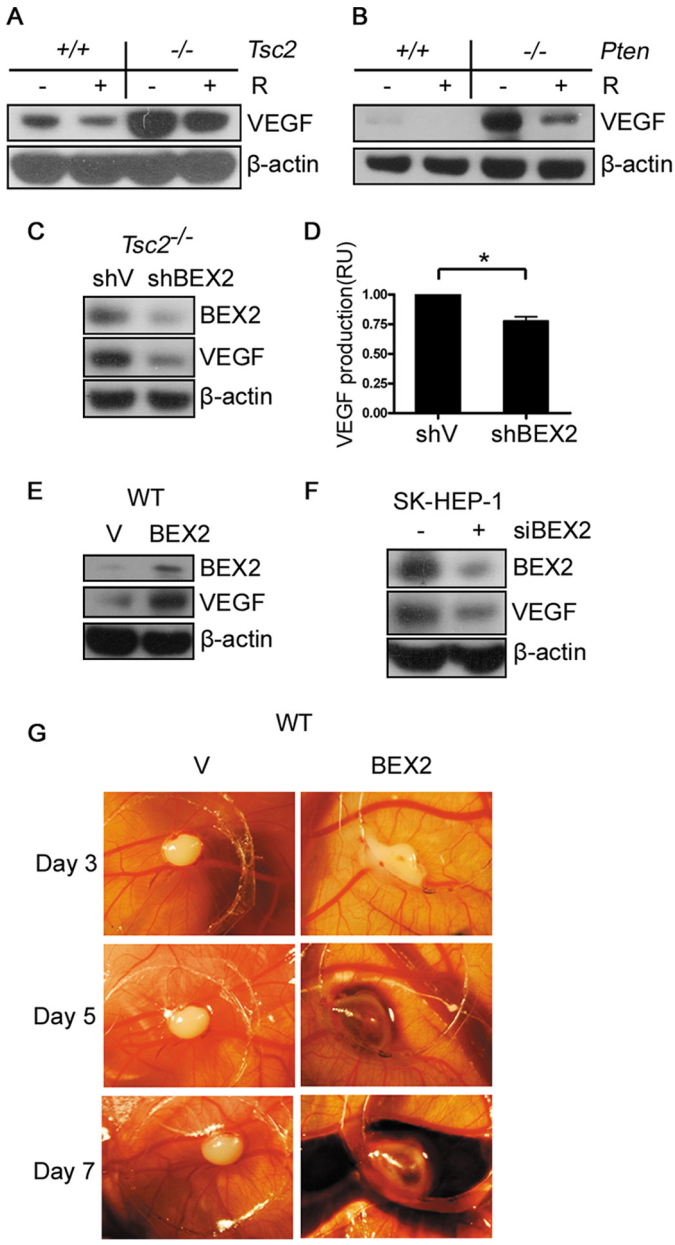

FIGURE 5. **mTOR enhances VEGF expression through up-regulation of BEX2.** *A* and *B*, WT and *Tsc2*$^{-/-}$ MEFs (*A*) or *Pten*$^{-/-}$ MEFs (*B*) were treated with or without 10 nM rapamycin (*R*) for 24 h and then subjected to immunoblotting. *C* and *D*, cell lysates were extracted from *Tsc2*$^{-/-}$ MEFs stably expressing the shRNA for BEX2 for immunoblotting (*C*), and cell culture supernatants from these MEFs were analyzed for VEGF (*D*). *shV*, scramble shRNA. $n = 3$, data represent mean ± S.E. *, $p < 0.05$. *RU*, relative unit. *E*, WT MEFs transduced with the retroviruses for BEX2 in pLXIN-hyg or the control vector pLXIN-hyg (*V*) were subjected to immunoblotting. *F*, SK-HEP-1 cells were transfected with control or BEX2 siRNAs for 48 h and then subjected to immunoblotting. *G*, WT MEFs transduced with the retroviruses for BEX2 expression in pLXIN-hyg or the control vector pLXIN-hyg (*V*) were subjected to the chick chorioallantoic membrane assay.

newly identified mTOR regulation of STAT3/NF-κB-BEX2-VEGF signaling network is present both *in vitro* and *in vivo*. Inhibition of mTOR by rapamycin down-regulated p-S6, p-STAT3, p-p65, BEX2, and VEGF in HepG2, SK-HEP-1, ELT3, and A549 cells (Fig. 6*C*). Moreover, there are concurrent increases in the protein levels of p-S6, p-STAT3, p-p65, BEX2, and VEGF in kidney cystadenomas of four *Tsc2*$^{+/-}$ mice when compared with that in paratumor tissues (Fig. 6*D*). Taken

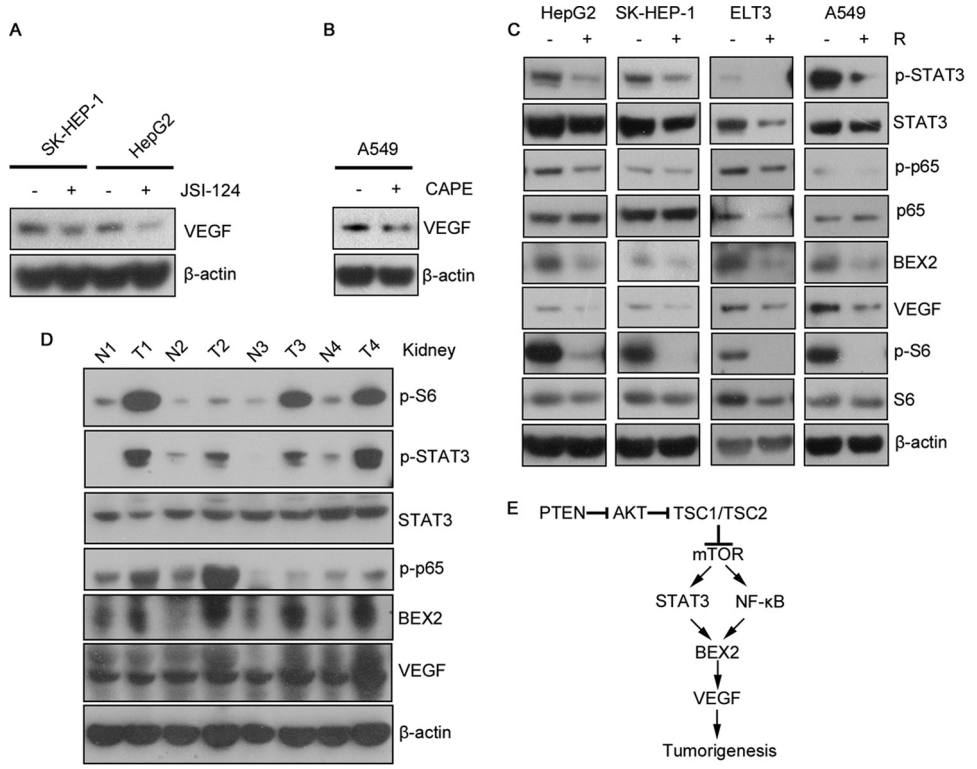

FIGURE 6. **mTOR regulates STAT3/NF-κB-BEX2-VEGF signaling *in vitro* and *in vivo*.** *A*, SK-HEP-1 and HepG2 cells were treated with or without 0.1 μM JSI-124 for 24 h and then subjected to immunoblotting. *B*, A549 cells were treated with or without 10 μM CAPE for 24 h and then subjected to immunoblotting. *C*, HepG2, SK-HEP-1, ELT3, and A549 cells were treated with or without 10 nM rapamycin (*R*) for 24 h and then subjected to immunoblotting. *D*, kidney cystadenomas (*T*) and paratumor tissues (*N*) from four C57BL/6 *Tsc2*$^{+/-}$ mice were harvested and then subjected to immunoblotting. *E*, schematic representation of the regulation of PTEN-AKT-TSC1/2-mTOR-STAT3/NF-κB-BEX2-VEGF signaling pathway in tumorigenesis. Hyperactive mTOR augments BEX2 expression through activation of both STAT3 and NF-κB, and the subsequent up-regulation of BEX2 increases VEGF and ultimately promotes tumorigenesis.

together, these data indicate that the mTOR-STAT3/NF-κB-BEX2-VEGF signaling network exists *in vitro* and *in vivo*.

Discussion

RTK-PI3K/PTEN-AKT-TSC1/2-mTOR signaling pathway is frequently deregulated in cancer, but the underlying mechanisms remain less clear. In this study, we have elucidated that BEX2 is a novel downstream target of mTOR, and activation of mTOR promotes tumorigenesis through up-regulation of STAT3/NF-κB-BEX2-VEGF signaling cassette.

As the significance of mTOR signaling in physiology and diseases has been increasingly appreciated, the molecular events downstream of mTOR are under intensive investigation. In addition, the underlying mechanism of mTOR up-regulation of angiogenesis is not completely understood. Evidence has shown that BEX2 is overexpressed in breast cancer (20), indicating that BEX2 may play a role in cancer development. Reduction of BEX2 expression inhibits angiogenesis *in vivo* (22). Our microarray analysis revealed that the abundance of BEX2 was ~8.5-fold higher in *Tsc2*$^{-/-}$ MEFs than in WT MEFs (Table 1). Therefore, BEX2 was chosen for mechanistic study of tumorigenesis caused by aberrant activation of mTOR.

By studying *Tsc2*$^{-/-}$ MEFs, *Pten*$^{-/-}$ MEFs, rat *Tsc2* mutant uterine leiomyoma cells, human cancer cell lines, neuronal specific *Tsc1* knock-out mice, hepatic specific *Pten* knock-out mice, heterozygous *Tsc2* deletion mice, and a TSC patient, we have found that negative regulation of BEX2 expression by PTEN or TSC2 is mediated by mTORC1 (Figs. 1 and 2). Because the abundance of BEX2 is higher in TSC-associated kidney angiomyolipoma, the enhanced expression of BEX2 may be involved in TSC development. We speculate that BEX2 is a candidate target for the treatment of TSC.

There is limited characterization on the regulatory mechanisms upstream of BEX2. Our data show that STAT3, a downstream effector of mTOR, is a positive regulator of BEX2, and BEX2 is thus a novel effector of STAT3. Moreover, STAT3 up-regulates BEX2 expression by directly binding to the promoter of BEX2 gene (Fig. 4, *A–F*). In addition, NF-κB positively regulates BEX2 expression. However, NF-κB does not influence the transcription of BEX2 gene (Fig. 4, *G–I*), and therefore NF-κB regulation of BEX2 is likely a post-transcriptional event. Based on our previous study (25) and the finding in this study (Fig. 4*J*), there is no functional cross-talk between STAT3 and NF-κB. We propose that STAT3 and NF-κB positively modulate BEX2 expression downstream of mTOR in parallel.

The role of BEX2 in tumorigenesis is controversial. BEX2 is considered as a proto-oncogene in breast cancer (21) and a tumor suppressor in glioma (24). Our data demonstrate that reduction of BEX2 inhibits tumorigenesis of *Tsc2*$^{-/-}$ or *Pten*$^{-/-}$ MEFs (Fig. 3), supporting BEX2 as an mTOR-regulated proto-oncogene. Thus, BEX2 is a promising target that may be harnessed for the treatment of cancers associated with aberrant mTOR signaling.

It is well known that hyperactive mTOR signaling leads to tumorigenesis with augmented angiogenesis, and VEGF has

been established as a major stimulator of angiogenesis (18, 47). Here we have demonstrated that BEX2, as a novel downstream target of mTOR, positively controls VEGF expression, and BEX2 overexpression in WT MEFs promotes angiogenesis in the chick chorioallantoic membrane (Fig. 5). STAT3 and NF-κB augment BEX2 expression induced by mTOR (Fig. 4). Moreover, STAT3 and NF-κB are positive upstream regulators of VEGF (Fig. 6, *A* and *B*). In addition, the mTOR-STAT3/NF-κB-BEX2-VEGF signaling cascade was shown to exist in human cancer cell lines *in vitro* and renal tumors of $Tsc2^{+/-}$ mice *in vivo* (Fig. 6, *C* and *D*). Taken together, mTOR may promote tumorigenesis through enhanced STAT3/NF-κB-BEX2-VEGF signaling cassette (Fig. 6*E*). As a target gene of c-Jun, BEX2 reciprocally regulates c-Jun in breast cancer (48). mTOR signaling pathway augments VEGF expression through up-regulation of HIF-1α (18, 49). c-Jun positively regulates VEGF expression by stabilizing HIF-1α (50). Hence, we postulate BEX2 enhances VEGF through up-regulation of c-Jun-HIF-1α signaling cascade.

In summary, we have illustrated that BEX2 plays an important role in tumorigenesis caused by aberrant activation of mTOR. Hyperactivation of mTOR stimulates STAT3/NF-κB-BEX2-VEGF signaling cascade. The components in the newly established mTOR-STAT3/NF-κB-BEX2-VEGF cascade are potential targets for the treatment of cancer with aberrant RTK-PI3K/PTEN-AKT-TSC1/2-mTOR signaling.

Author Contributions—Z. H. designed and carried out most of the experiments, analyzed data, and wrote most of the paper. Y. W. performed experiments, analyzed data, and revised the paper. F. H. performed experiments and analyzed data. R. C. provided human kidney tumor tissue samples. C. L. provided ELT-3 cells stably expressing TSC2. F. W. performed the gene expression profiling analysis. J. G. and D. J. K. provided brain tissues of neuronal specific Tsc1 knockout and WT control mice. J. L. and J. W. B. performed chick chorioallantoic membrane assay for angiogenesis. P. T. supervised some of the study. H. Z. and X. Z. designed experiments, analyzed data, and wrote the paper.

Acknowledgments—We thank Xinxin Chen and Yanling Jing for technical assistance and insightful discussion.

References

1. Manning, B. D., and Cantley, L. C. (2007) AKT/PKB signaling: navigating downstream. *Cell* **129,** 1261–1274
2. Guertin, D. A., and Sabatini, D. M. (2007) Defining the role of mTOR in cancer. *Cancer Cell* **12,** 9–22
3. Eng, C. (2003) *PTEN*: one gene, many syndromes. *Hum. Mutat.* **22,** 183–198
4. Di Cristofano, A., and Pandolfi, P. P. (2000) The multiple roles of PTEN in tumor suppression. *Cell* **100,** 387–390
5. Inoki, K., Li, Y., Zhu, T., Wu, J., and Guan, K. L. (2002) TSC2 is phosphorylated and inhibited by Akt and suppresses mTOR signalling. *Nat. Cell Biol.* **4,** 648–657
6. Crino, P. B., Nathanson, K. L., and Henske, E. P. (2006) The tuberous sclerosis complex. *N. Engl. J. Med.* **355,** 1345–1356
7. Hay, N., and Sonenberg, N. (2004) Upstream and downstream of mTOR. *Genes Dev.* **18,** 1926–1945
8. Albert, V., and Hall, M. N. (2015) mTOR signaling in cellular and organismal energetics. *Curr. Opin. Cell Biol.* **33,** 55–66
9. Wang, S., Tsun, Z. Y., Wolfson, R. L., Shen, K., Wyant, G. A., Plovanich, M. E., Yuan, E. D., Jones, T. D., Chantranupong, L., Comb, W., Wang, T., Bar-Peled, L., Zoncu, R., Straub, C., Kim, C., Park, J., Sabatini, B. L., and Sabatini, D. M. (2015) Lysosomal amino acid transporter SLC38A9 signals arginine sufficiency to mTORC1. *Science* **347,** 188–194
10. Jewell, J. L., Kim, Y. C., Russell, R. C., Yu, F. X., Park, H. W., Plouffe, S. W., Tagliabracci, V. S., and Guan, K. L. (2015) Differential regulation of mTORC1 by leucine and glutamine. *Science* **347,** 194–198
11. Kim, D. H., Sarbassov, D. D., Ali, S. M., King, J. E., Latek, R. R., Erdjument-Bromage, H., Tempst, P., and Sabatini, D. M. (2002) mTOR interacts with raptor to form a nutrient-sensitive complex that signals to the cell growth machinery. *Cell* **110,** 163–175
12. Alessi, D. R., Pearce, L. R., and García-Martínez, J. M. (2009) New insights into mTOR signaling: mTORC2 and beyond. *Sci. Signal.* **2,** pe27
13. Kwiatkowski, D. J., Whittemore, V. H., and Thiele, E. A. (2010) *Tuberous Sclerosis Complex: Genes, Clinical Features and Therapeutics*, Weinheim, Germany: Wiley-Blackwell
14. Kondo, S., Asano, M., Matsuo, K., Ohmori, I., and Suzuki, H. (1994) Vascular endothelial growth factor/vascular permeability factor is detectable in the sera of tumor-bearing mice and cancer patients. *Biochim. Biophys. Acta* **1221,** 211–214
15. Ferrara, N., and Davis-Smyth, T. (1997) The biology of vascular endothelial growth factor. *Endocr. Rev.* **18,** 4–25
16. El-Hashemite, N., Walker, V., Zhang, H., and Kwiatkowski, D. J. (2003) Loss of *Tsc1* or *Tsc2* induces vascular endothelial growth factor production through mammalian target of rapamycin. *Cancer Res.* **63,** 5173–5177
17. Brugarolas, J. B., Vazquez, F., Reddy, A., Sellers, W. R., and Kaelin, W. G., Jr. (2003) TSC2 regulates VEGF through mTOR-dependent and -independent pathways. *Cancer Cell* **4,** 147–158
18. Karar, J., and Maity, A. (2011) PI3K/AKT/mTOR pathway in angiogenesis. *Front. Mol. Neurosci.* **4,** 51
19. Alvarez, E., Zhou, W., Witta, S. E., and Freed, C. R. (2005) Characterization of the Bex gene family in humans, mice, and rats. *Gene* **357,** 18–28
20. Naderi, A., Teschendorff, A. E., Beigel, J., Cariati, M., Ellis, I. O., Brenton, J. D., and Caldas, C. (2007) *BEX2* is overexpressed in a subset of primary breast cancers and mediates nerve growth factor/nuclear factor-κB inhibition of apoptosis in breast cancer cell lines. *Cancer Res.* **67,** 6725–6736
21. Naderi, A., Liu, J., and Bennett, I. C. (2010) BEX2 regulates mitochondrial apoptosis and G_1 cell cycle in breast cancer. *Int. J. Cancer* **126,** 1596–1610
22. Le Mercier, M., Fortin, S., Mathieu, V., Roland, I., Spiegl-Kreinecker, S., Haibe-Kains, B., Bontempi, G., Decaestecker, C., Berger, W., Lefranc, F., and Kiss, R. (2009) Galectin 1 proangiogenic and promigratory effects in the Hs683 oligodendroglioma model are partly mediated through the control of *BEX2* expression. *Neoplasia* **11,** 485–496
23. Zhou, X., Xu, X., Meng, Q., Hu, J., Zhi, T., Shi, Q., and Yu, R. (2013) Bex2 is critical for migration and invasion in malignant glioma cells. *J. Mol. Neurosci.* **50,** 78–87
24. Foltz, G., Ryu, G. Y., Yoon, J. G., Nelson, T., Fahey, J., Frakes, A., Lee, H., Field, L., Zander, K., Sibenaller, Z., Ryken, T. C., Vibhakar, R., Hood, L., and Madan, A. (2006) Genome-wide analysis of epigenetic silencing identifies *BEX1* and *BEX2* as candidate tumor suppressor genes in malignant glioma. *Cancer Res.* **66,** 6665–6674
25. Ma, J., Meng, Y., Kwiatkowski, D. J., Chen, X., Peng, H., Sun, Q., Zha, X., Wang, F., Wang, Y., Jing, Y., Zhang, S., Chen, R., Wang, L., Wu, E., Cai, G., Malinowska-Kolodziej, I., Liao, Q., Liu, Y., Zhao, Y., Sun, Q., Xu, K., Dai, J., Han, J., Wu, L., Zhao, R. C., Shen, H., and Zhang, H. (2010) Mammalian target of rapamycin regulates murine and human cell differentiation through STAT3/p63/Jagged/Notch cascade. *J. Clin. Invest.* **120,** 103–114
26. Kobayashi, T., Hirayama, Y., Kobayashi, E., Kubo, Y., and Hino, O. (1995) A germline insertion in the tuberous sclerosis (*Tsc2*) gene gives rise to the Eker rat model of dominantly inherited cancer. *Nat. Genet.* **9,** 70–74
27. Zha, X., Hu, Z., Ji, S., Jin, F., Jiang, K., Li, C., Zhao, P., Tu, Z., Chen, X., Di, L., Zhou, H., and Zhang, H. (2015) NFκB up-regulation of glucose transporter 3 is essential for hyperactive mammalian target of rapamycin-induced aerobic glycolysis and tumor growth. *Cancer Lett.* **359,** 97–106
28. Zhang, H., Bajraszewski, N., Wu, E., Wang, H., Moseman, A. P., Dabora, S. L., Griffin, J. D., and Kwiatkowski, D. J. (2007) PDGFRs are critical for PI3K/Akt activation and negatively regulated by mTOR.

J. Clin. Invest. **117,** 730–738
29. Bromberg, J. F., Horvath, C. M., Besser, D., Lathem, W. W., and Darnell, J. E., Jr. (1998) Stat3 activation is required for cellular transformation by v-*src*. *Mol. Cell. Biol.* **18,** 2553–2558
30. Finlay, G. A., York, B., Karas, R. H., Fanburg, B. L., Zhang, H., Kwiatkowski, D. J., and Noonan, D. J. (2004) Estrogen-induced smooth muscle cell growth is regulated by tuberin and associated with altered activation of platelet-derived growth factor receptor-β and ERK-1/2. *J. Biol. Chem.* **279,** 23114–23122
31. Sun, Q., Chen, X., Ma, J., Peng, H., Wang, F., Zha, X., Wang, Y., Jing, Y., Yang, H., Chen, R., Chang, L., Zhang, Y., Goto, J., Onda, H., Chen, T., Wang, M. R., Lu, Y., You, H., Kwiatkowski, D., and Zhang, H. (2011) Mammalian target of rapamycin up-regulation of pyruvate kinase isoenzyme type M2 is critical for aerobic glycolysis and tumor growth. *Proc. Natl. Acad. Sci. U.S.A.* **108,** 4129–4134
32. Peng, H., Liu, J., Sun, Q., Chen, R., Wang, Y., Duan, J., Li, C., Li, B., Jing, Y., Chen, X., Mao, Q., Xu, K. F., Walker, C. L., Li, J., Wang, J., and Zhang, H. (2013) mTORC1 enhancement of STIM1-mediated store-operated Ca^{2+} entry constrains tuberous sclerosis complex-related tumor development. *Oncogene* **32,** 4702–4711
33. Hagedorn, M., Javerzat, S., Gilges, D., Meyre, A., de Lafarge, B., Eichmann, A., and Bikfalvi, A. (2005) Accessing key steps of human tumor progression *in vivo* by using an avian embryo model. *Proc. Natl. Acad. Sci. U.S.A.* **102,** 1643–1648
34. Onda, H., Lueck, A., Marks, P. W., Warren, H. B., and Kwiatkowski, D. J. (1999) *Tsc2*$^{+/-}$ mice develop tumors in multiple sites that express gelsolin and are influenced by genetic background. *J. Clin. Invest.* **104,** 687–695
35. Meikle, L., Talos, D. M., Onda, H., Pollizzi, K., Rotenberg, A., Sahin, M., Jensen, F. E., and Kwiatkowski, D. J. (2007) A mouse model of tuberous sclerosis: neuronal loss of Tsc1 causes dysplastic and ectopic neurons, reduced myelination, seizure activity, and limited survival. *J. Neurosci.* **27,** 5546–5558
36. Horie, Y., Suzuki, A., Kataoka, E., Sasaki, T., Hamada, K., Sasaki, J., Mizuno, K., Hasegawa, G., Kishimoto, H., Iizuka, M., Naito, M., Enomoto, K., Watanabe, S., Mak, T. W., and Nakano, T. (2004) Hepatocyte-specific Pten deficiency results in steatohepatitis and hepatocellular carcinomas. *J. Clin. Invest.* **113,** 1774–1783
37. Wang, Y., Hu, Z., Liu, Z., Chen, R., Peng, H., Guo, J., Chen, X., and Zhang, H. (2013) MTOR inhibition attenuates DNA damage and apoptosis through autophagy-mediated suppression of CREB1. *Autophagy* **9,** 2069–2086
38. Johnston, P. A., and Grandis, J. R. (2011) STAT3 signaling: anticancer strategies and challenges. *Mol. Interv.* **11,** 18–26
39. Bromberg, J. F., Wrzeszczynska, M. H., Devgan, G., Zhao, Y., Pestell, R. G., Albanese, C., and Darnell, J. E., Jr. (1999) *Stat3* as an oncogene. *Cell* **98,** 295–303
40. Zha, X., Wang, F., Wang, Y., He, S., Jing, Y., Wu, X., and Zhang, H. (2011) Lactate dehydrogenase B is critical for hyperactive mTOR-mediated tumorigenesis. *Cancer Res.* **71,** 13–18
41. Ghosh, S., and Karin, M. (2002) Missing pieces in the NF-κB puzzle. *Cell* **109,** (suppl.) S81–S96, 10.1016/S0092-8674(02)00703-1
42. Karin, M., and Lin, A. (2002) NF-κB at the crossroads of life and death. *Nat. Immunol.* **3,** 221–227
43. Dan, H. C., Cooper, M. J., Cogswell, P. C., Duncan, J. A., Ting, J. P., and Baldwin, A. S. (2008) Akt-dependent regulation of NF-κB is controlled by mTOR and Raptor in association with IKK. *Genes Dev.* **22,** 1490–1500
44. Fang, J., Ding, M., Yang, L., Liu, L. Z., and Jiang, B. H. (2007) PI3K/PTEN/AKT signaling regulates prostate tumor angiogenesis. *Cell. Signal.* **19,** 2487–2497
45. Xu, Q., Briggs, J., Park, S., Niu, G., Kortylewski, M., Zhang, S., Gritsko, T., Turkson, J., Kay, H., Semenza, G. L., Cheng, J. Q., Jove, R., and Yu, H. (2005) Targeting Stat3 blocks both HIF-1 and VEGF expression induced by multiple oncogenic growth signaling pathways. *Oncogene* **24,** 5552–5560
46. Fujioka, S., Niu, J., Schmidt, C., Sclabas, G. M., Peng, B., Uwagawa, T., Li, Z., Evans, D. B., Abbruzzese, J. L., and Chiao, P. J. (2004) NF-κB and AP-1 connection: mechanism of NF-κB-dependent regulation of AP-1 activity. *Mol. Cell. Biol.* **24,** 7806–7819
47. Carmeliet, P., and Jain, R. K. (2000) Angiogenesis in cancer and other diseases. *Nature* **407,** 249–257
48. Naderi, A., Liu, J., and Hughes-Davies, L. (2010) BEX2 has a functional interplay with c-Jun/JNK and p65/RelA in breast cancer. *Mol. Cancer* **9,** 111
49. Zhong, H., Chiles, K., Feldser, D., Laughner, E., Hanrahan, C., Georgescu, M. M., Simons, J. W., and Semenza, G. L. (2000) Modulation of hypoxia-inducible factor 1α expression by the epidermal growth factor/phosphatidylinositol 3-kinase/PTEN/AKT/FRAP pathway in human prostate cancer cells: implications for tumor angiogenesis and therapeutics. *Cancer Res.* **60,** 1541–1545
50. Yu, B., Miao, Z. H., Jiang, Y., Li, M. H., Yang, N., Li, T., and Ding, J. (2009) c-Jun protects hypoxia-inducible factor-1α from degradation via its oxygen-dependent degradation domain in a nontranscriptional manner. *Cancer Res.* **69,** 7704–7712